INTERNATIONAL JOURNAL OF INNOVATIVE RESEARCH & DEVELOPMENT

ISSN 2278 – 0211 (Online)

Assessment of the Saline-Water Intrusion through the Fresh Groundwater Aquifer by Using ER and TEM Methods at the Qantara Shark Area, Sinai Peninsula, Egypt

A. A. Basheer
Geomagnetic and Geoelectric Department
National Research Institute of Astronomy and Geophysics, Helwan, Cairo, Egypt
A. I. Taha
Geomagnetic and Geoelectric Department
National Research Institute of Astronomy and Geophysics, Helwan, Cairo, Egypt
Kh. Q. Mansour
Geomagnetic and Geoelectric Department
National Research Institute of Astronomy and Geophysics, Helwan, Cairo, Egypt
A. Khalil
Geomagnetic and Geoelectric Department
National Research Institute of Astronomy and Geophysics, Helwan, Cairo, Egypt
T. Rabeh
Geomagnetic and Geoelectric Department
National Research Institute of Astronomy and Geophysics, Helwan, Cairo, Egypt

Abstract:
One of the most famous problem faces the coastal agricultural area is the saline-water intrusion from sea. This study endeavors at detailing the prevailing subsurface conditions from the viewpoint of groundwater location, depth and quality. Two well-known geophysical methods have been used and applied to determine the depth of the fresh water aquifer and the saline water intrusion. The vertical electrical sounding and time-domain electromagnetic sounding have been pertained in the same 67 sites, which covers the study area. Analysis and interpretation of the obtained results reveals that, the subsurface consists of three geo-electrical layers with a gentle general slope towards the sea. The fresh water overlies saline water. It deserves mention to note that the fresh water depth varies between 0.5 and 65 m. under the ground surface. The saline water depth varies between 23 and 83 m. below the ground surface.

Key words: *ER; TEM; Saline water intrusion; Fresh water aquifer; Qantar Shark Area; Sinai Peninsula, Egypt*

1. Introduction

Qantara Shark "West Arch" is one of the famous newest agriculture areas in north Sinai. The study area takes palace over 200 kilometers in Latitude ranges between 30.851° and 31.299° and Longitude ranges between 32.249° and 32.796° (Figure 1). The study area considers as the extended west bank of the delta, in spite of the Suez Canal separates it from the east Delta and affiliates it with the Sinai Peninsula.

The main targets of this study area are to determine the water table and the groundwater aquifer in the study area. Details electric and electromagnetic study had been carried out by making sixty seven of Current Vertical Electrical Sounding [CVES] and sixty seven of Time-Domain Electromagnetic Sounding [TEM] covered the study .Figure (3) shows the elevation above sea level and the distribution of both CVES and TEM sites in the study area.

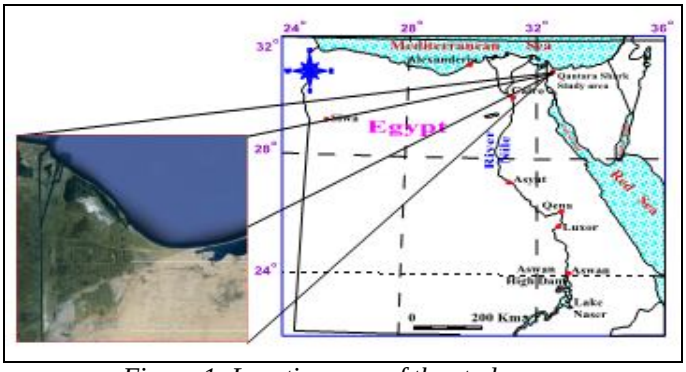

Figure 1: Location map of the study area

2. Geomorphologic and Geologic Setting

Northwest Sinai locates within the semi-arid belt of Egypt. This aridity manifests by the occurrence of sand dunes and sand sheets, salt marshes and ponds as well as lack of vegetation. Geomorphologically, northwestern Sinai embodies five distinctive units:

- Coastal area, which includes old shore, coastal sand dunes, the strand plain of successive beach ridges with intervening runnels recording shoreline progradation during Late Holocene, and deltaic plain covered by mouth bar and distributaries channel fill sands (El-Asmar, 1999);
- El-Bardawil Lagoon;
- Aeolian sand which covers the majority of north Sinai and consists of wind-laid sediments including aeolian siliclastic sabkhas (Assal, 1999);
- Mobile sand dunes; and
- Salt marshes and sabkhas (inland sabkhas and coastal sabkhas).

Geologically, northwestern Sinai is covered by Quaternary deposits Figure (2). The Pleistocene deposits include: Sahl El-Tineh Formation which consists of a mixture of black and white sands with silt, Al- Qantara Formation which consists of sand and grits with minor clay interbeds, coquina deposits, canglomerates, and alluvial hamadah deposits (Geological Survey of Egypt, 1992). According to GSE (1992), the Holocene deposits are classified into: coastal sand dunes which extend parallel to the Mediterranean Sea coast, inland sand dunes and sheets that cover large areas of northwestern Sinai (the main water bearing formation for groundwater), coastal and inland sabkhas, and interdunal playa deposits; consist of fine sand and silt associated with evaporates (Deiab, 1998).

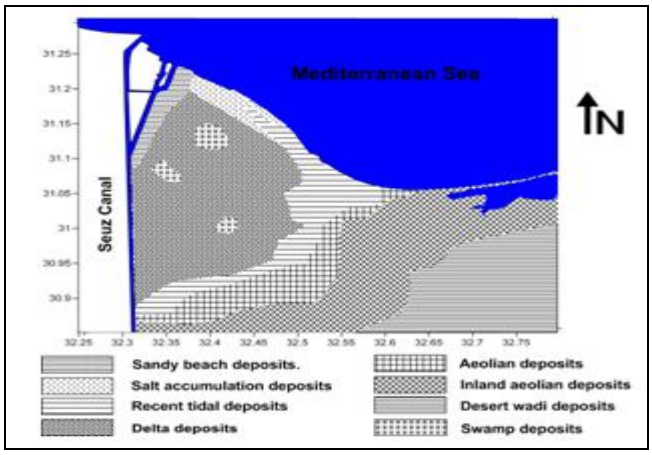

Figure 2: Geological map of the study area, after GSE (1992)

The study area level ranges from zero [sea level] to about 60 meters above sea level, the highest elevation values set in southwestern part of the study area and the lowest elevation values set in the north and southwest parts of the study area Figure (3).

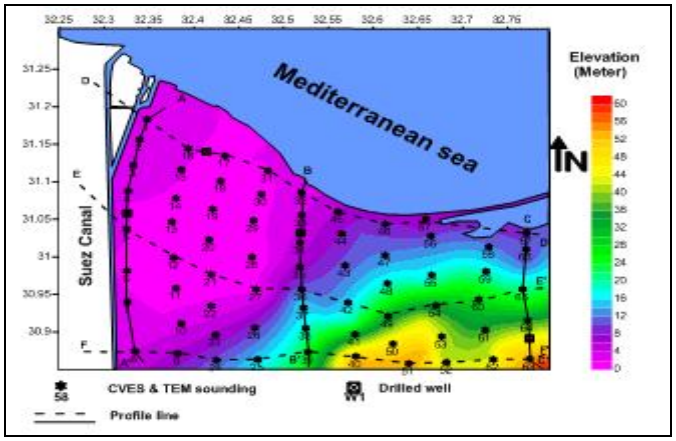

Figure 3: Elevation map of the study area with location of CVES, TEM soundings, drilled wells, and profiles' sites

3. Applied Geophysical Methods

3.1. The Electrical Resistivity Method

This study used the Syscal/R2 acquisition system to measure 67 VES'es distributes over the studied area (Figure (3)) to reveal the subsurface geoelectrical layers in the studied area. In field application, four-point configurations are used to measure the resistivity of the ground (Figure (4)).

Current is injected through two electrodes, by convention referees to as A and B, with two additional electrodes M and N, the voltage Vmn between two points can be measured. From the input current intensity (I), the measured voltage Vmn and the distribution of the electrodes, the apparent resistivity of the underground can be calculated as:

$$\rho = 2 \pi K \frac{Vmn}{I} \quad (1)$$

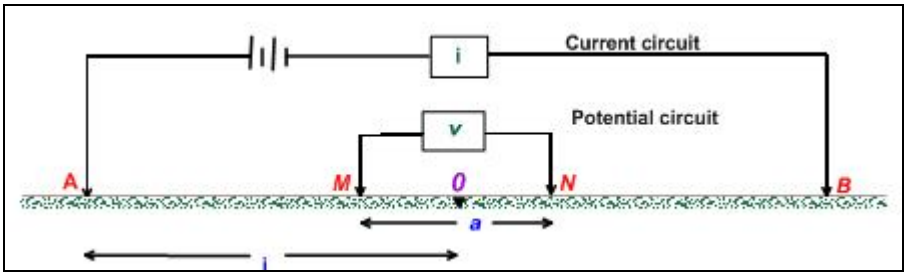

Figure 4: (a) Current lines and equip-potentials for a pair of current electrodes A and B on a homogeneous half-sp e. ac. (b) Schlumberger electrode arrangement used in DC resistivity surveying

Where, K is the array geometric factor, which depends on the electrode configuration.

In Schlumberger sounding, the potential electrodes are set at a certain separation and the current electrodes are moved symmetrically outward until the voltages become too small to be measured.

3.2. TEM Sounding Method

Transient sounding is typically made using non-grounded squared loops for transmitter and receiver antennas. The steady transmitter current produces a primary magnetic field, which is directed upward inside the loop and downward outside the loop. When the transmitter current is abruptly turned off, current is induced in the ground, which tries to maintain the magnetic field, which was presented prior to turn off. The magnetic field produced by the induced current is called the secondary magnetic field. The induced current will flow in horizontal circles under the transmitter loop.

Initially the current is concentrated near the surface, but as time passes the maximum current density moves downward and outward (Nabighian, 1979). The diffusion and dissipation of the current density are controlled by the resistivity of the ground. The more resistive the ground, the faster the maximum current diffuses downward, and the more rapid the dissipation of the current. For a loge red earth, the current will reside longer in conductive zones than in resistive zones of similar thickness (Hoversten et al., 1982).

Because the induced current is controlled by the resistivity structure of the material beneath the loop, the secondary magnetic field produced by this current system can be measured to determine the geoelectrical section (Fitterman, 1986a&b).

3.2.1. Time-Domain Electromagnetic Conductivity Meter

SIROTEM MK3 instrument, which is made in Australia, is used in this study. SIROTEM stands for Scientific Industrial Research Organization TEM. SIROTEM MK3 detects underground conducting materials by transmitting electrical pulses along loops of cable laid out on the surface. It is unique in having the transmitter and receiver in a single unit. The major components of SIROTEM MK3 are contained in a robust, portable console unit.

3.2.2. Physical Basis For TEM Sounding

TEM soundings are made with a receiver and transmitter unit attached to a receiver and a large transmitter loop. The transmitter passes a constant current through the loop, which produces a primary magnetic field (Figure 5). The current is quickly turned off, there by interrupting the primary magnetic field. To satisfy Faraday's law, currents are induced in the ground, which instantaneously maintain the primary magnetic field. This current system, which flows in closed paths below the transmitter loop, produces a secondary magnetic field. Changes of the secondary magnetic field with time induce a voltage in the receiver, because the magnitude and distribution of the current intensity depend upon the resistivity of the ground, the voltage gives information about the resistivity of the ground. The locus of the maximum amplitude of the induced currents diffuses downward and outward with time, thereby giving information about deeper regions as time increases (Nabighian, 1979). The signal recorded by the receiver is called a transient.

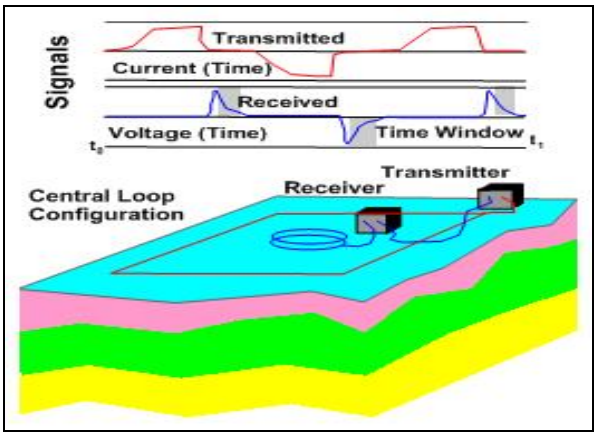

Figure 5: TEM system in central-loop configuration and the transmitted and received TEM waveforms

4. Data Interpretation

4.1. CVES Data Processing

The apparent resistivity data that collected from the field are processed by Zohdy (1989) and Resist (1990) software. The interpreted data came in true resistivity value and thickness of every layer. An example of these interpretations is shown in figure (6).

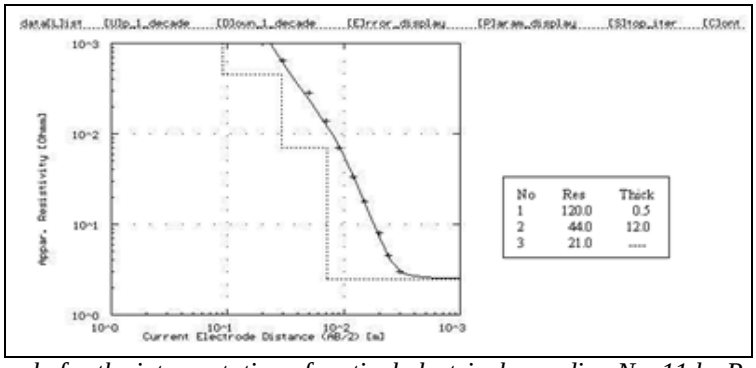

Figure 6: Example for the interpretation of vertical electrical sounding No. 11 by Resist's software

4.2. TEM (Time Domain) Data Processing

There are many ways in which TEM data can be processed and these are largely dependent upon which instrument system is used to acquire the original data. Most TEM systems record the transient voltage at a number of discrete intervals during the voltage decay, after the applied current is switched off. In each time the current is applied and then stopped, measurements are taken; when the current is applied again and switched off, a repeat set of measurements is taken. This process may be repeated many tens of times at a given location with all the data are being logged automatically. Consequently, these many data can be processed to improve the signal-to-noise ratio. At the same time, the field data are checked for repeatability.

Commonly, the data are normalized with respect to the transmitter current or other system parameter, and the effects of the time decay may be amplified in compensation by normalizing the observed field at each point with the respective primary field value at the same point.

Stephan et al. (1991) described a data processing sequence for long offset transient EM' (LOTEM) sounding undertaken in Germany. Three data processing stages are formulated:

- Pre-stack processing, was used to remove unwanted periodic noise using filtering such as a notch to remove noise associated with AC power lines. A selective stacking algorithm was applied to average only a percentage of the data around the median of the individual time samples. The consequence of this was to reduce the noise content. (Soliman M.M.2005)
- The post-stack processing was to apply a slight time variable smoothing filter. The culmination of this processing was the production of logarithmic plots of apparent resistivity as a function of decay time.

A variety of plots of processed data can be produced, such as transient decay (logarithmic) plots of voltage (in mV) versus decay time (in msec.), response profiles (graphs of measured voltage at a selected decay time at all stations in a survey area); response contours (the response profile data plotted in map form) and apparent resistivity plots, either as profiles or maps.

Interpretation methods are as varied as the different types of data plots and systems used to acquire the data. Typically, the interpretation is undertaken in two stages:

- The first is to locate a possible sub-surface target on the basis of the shape, size and location of the anomalies evident on profiles and maps of relevant parameters.
- The second, more quantitative, stage is to determine the quality of the conductor using time constants determined from decay plots of the field intensity at one or more locations.

Various types of display parameter are useful for different applications. For example apparent resistivity soundings can be extremely useful in hydrogeological investigation and in geological mapping but provide very little information appropriate for mineral exploration.

In this study, TEM soundings 49 stations have been carried out as a regional study in all studied area by using a SIROTEM time-domain system with 50 m x 50 m loop as a transmitter and receiver at the same time. The used "Delay times" are in the range 20 ms to 40 ms, and the used interpretation program is the TEMIXXL software (Interpex Ltd, USA) in interpretation. Figure (7) shows an example of TEM sounding interpretation result.

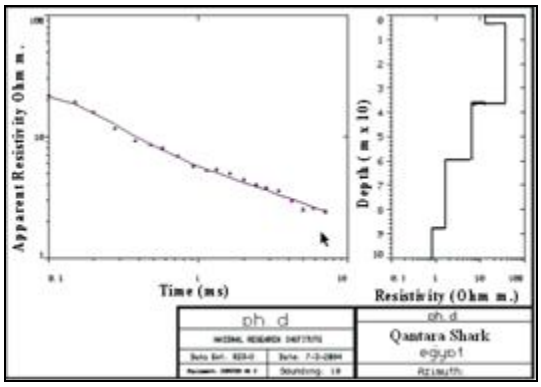

Figure 7: Example of interoperation of TEM sounding No. 34

5. Results

5.1. Cross-sections

Using the interpreted data which came out as true resistivities and thicknesses of the geo-electrical layers from the interpretation processing, six profiles have been drown to show the distribution of the layers. Three profiles have north–south direction; the other three ones went in east–west direction. It is clearly shown that the area consists of three layers, first layer has a lithology of Holocene Sands, the second Layer consists of Clay, and the third layer consists of Pleistocene Sands. The water table relies in depth under 0.5 m under the surface, but it changes in depth according to the covered layer and the elevation above the sea level to reach 45 m., saline water which seepages from the sea has depth varies from 23 m in the northern parts of the study area to 82 m. in the southern and southeastern parts of the study area. Figures from (8) to Figure (13) show these cross-sections with fresh water and saline water tables.

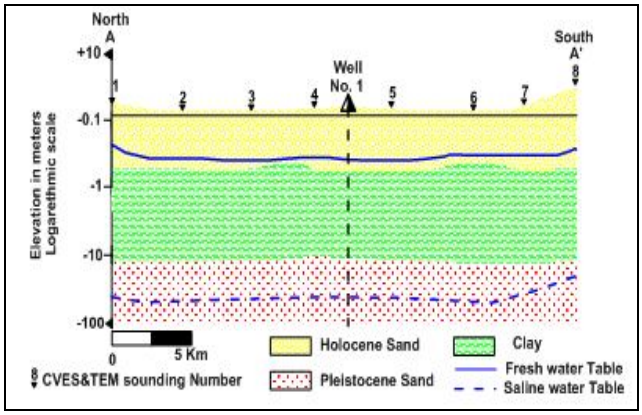

Figure (8): Geo-electrical Cross-section A-A'.

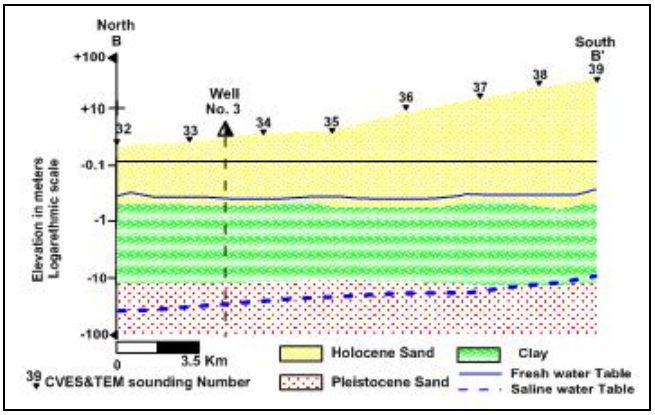

Figure (9): Geo-electrical Cross-section B-B'.

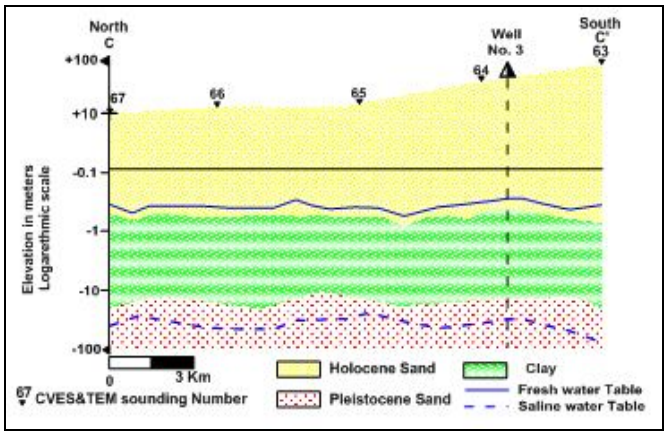

Figure (10): Geo-electrical Cross-section C-C'.

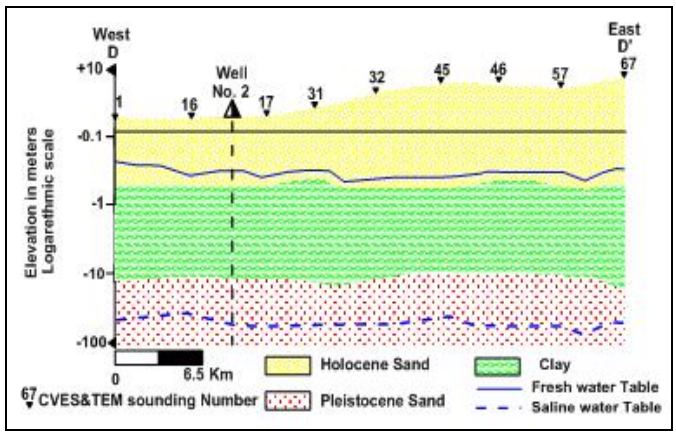

Figure (11): Geo-electrical Cross-section D-D'.

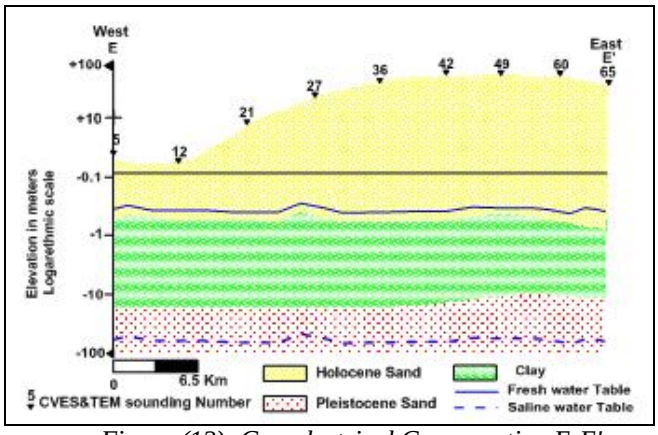

Figure (12): Geo-electrical Cross-section E-E'.

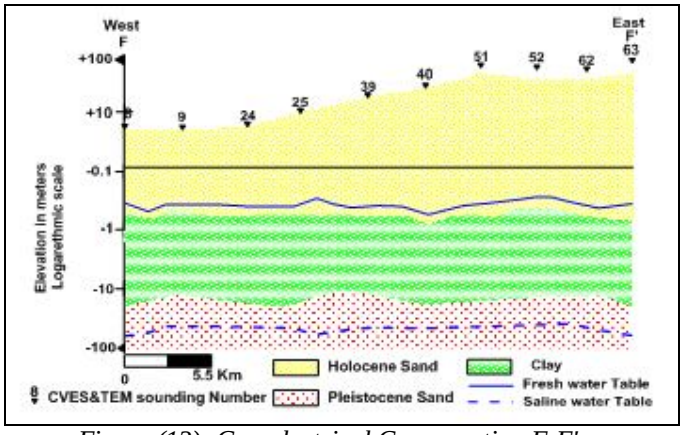

Figure (13): Geo-electrical Cross-section F-F'.

5.2. Maps

5.2.1. Resistivity Maps

The distribution of resistivity in the first "surface" layer has been drowning in map Figure (14). Resistivities of the surface layer show values range from 101 Ω.m. to 121 Ω.m. these values relate to the Holocene sands which saturate with sometimes with evaporated salt come from sea in the sea shore, figure (14) shows the distribution of these values in the surface layer over the study area. Figure (15) illustrates the resistivities of second layer demonstrate values between 44 Ω.m. to 80 Ω.m., these values can be relate to the fresh water in clay layer. The third layer illustrates resistivity values range from 20 Ω.m. to 35 Ω.m., these values may be relate to the lithology of Pleistocene sand formation with saline water in it Figure (16).

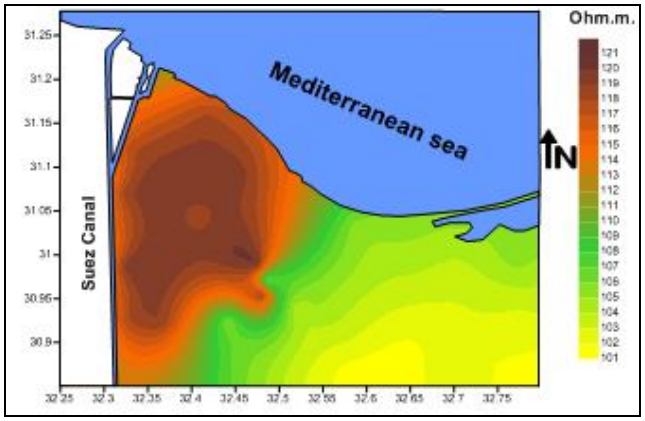

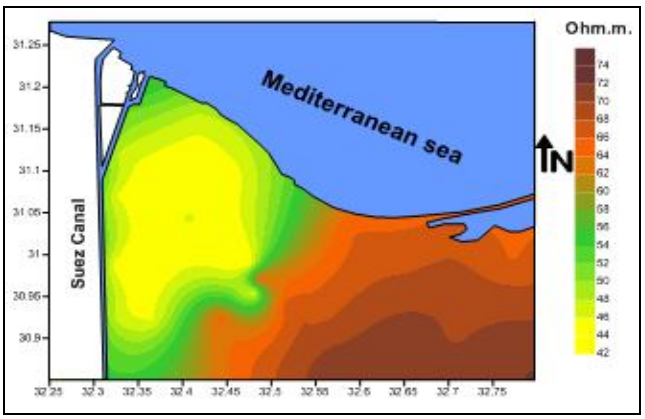

Figure 14: Resistivity map of the surface layer (Holocene sand) in the study area
Figure 15: Resistivity map of the second layer (Clay) in the study area

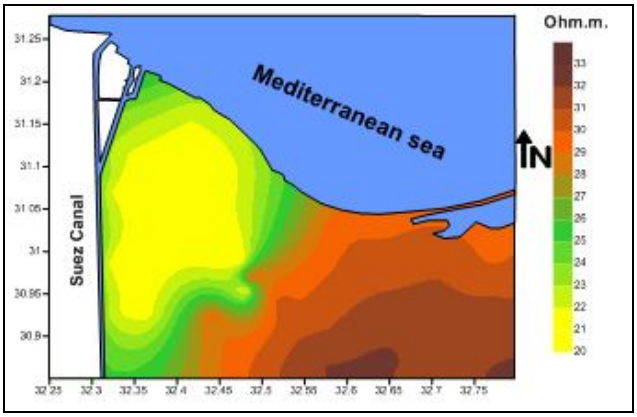

Figure 16: Resistivity map of the Third layer (Pleistocene sand) in the study area

5.2.2. Thickness Maps

Two thickness maps have been drowning. The first or surface layer, which consists of Holocene sand formation, varies in thick from about 1 m. to about 66 m. Figure (17). The second layer consists of clay and in some times intersected with shale lenses. This layer has thickness ranges from about 11 m. to about 13m., figure (18) shows the distribution of the thickness values of the second layer in the study area.

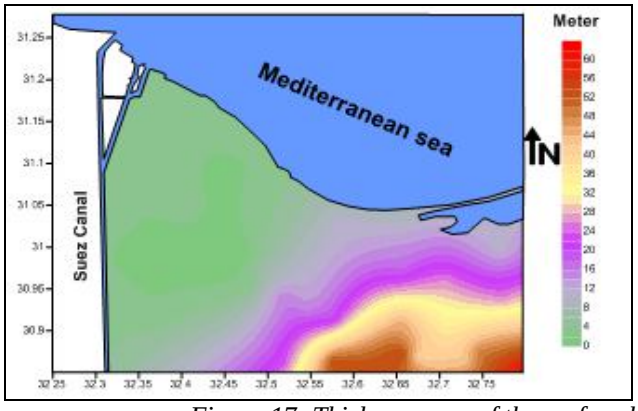

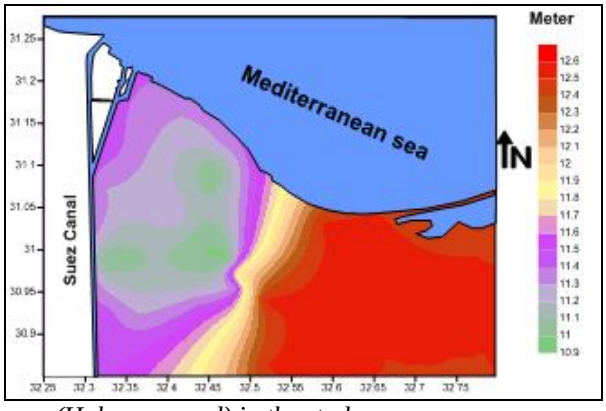

Figure 17: Thickness map of the surface layer (Holocene sand) in the study area
Figure 18: thickness map of the second layer (Clay) in the study area

5.2.3. Depth Maps

From the interpreted data, four depth maps has been drown, the first map in figure (19) shows the depth to the second layer, it can be clearly illustrated that this layer lies in depth ranges from 1 m. to about 66 m.., the most high depth values locate far from the sea shore in north of the study area to the southeastern parts.

The depth to the third layer has values between 10 m. and about 80 m. the high values present in the southeastern part of the study area, while the low values lie in the northern and the southwestern parts of the study area Figure (20).

The most important depth map shown in figure (21) that shows the depth to the fresh water table in the study area. Depth to fresh water ranges between 0.5 m. to 65 m. the shallow depth can be noted in the northern and southwestern parts of the study area. These values may be related to Delta groundwater's support and to the two man-made El-salam and Prince Gaber fresh water canals. These canals cross the study area from the west to the east in the middle and south of the area.

Figure (22) shows the depth to the saline water in the study area, this saline water intrudes by the sea and lies under the fresh water because of its density. The depth of this saline water ranges between 22 m. to 83 m.

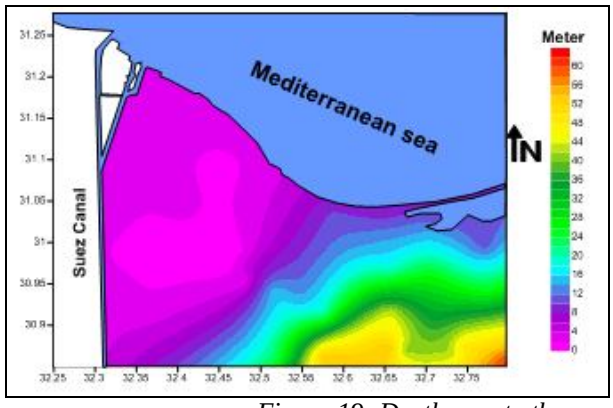

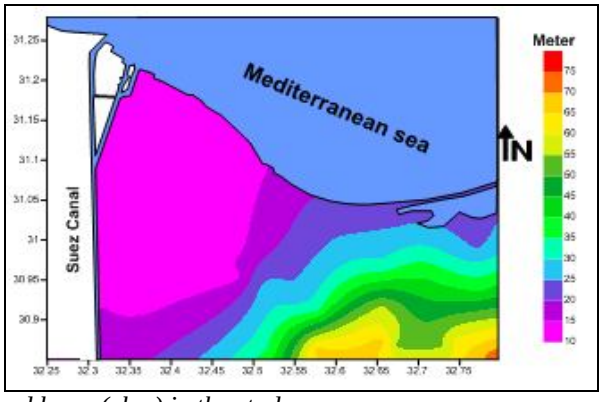

Figure 19: Depth map to the second layer (clay) in the study area

Figure 20: Depth map to the third layer (Pleistocene sand) in the study area

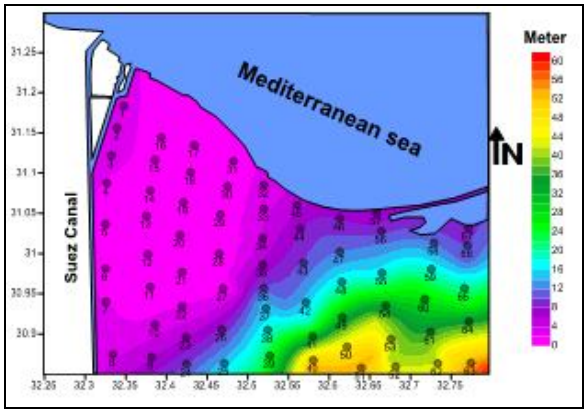

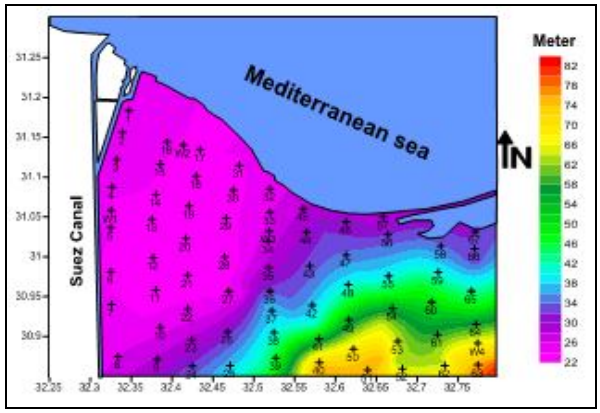

Figure 21: Depth map to the fresh water table in the study area with location of VES and TEM Soundings

Figure 22: Depth map to the saline water table in the study area with location of VES and TEM Soundings

6. Results and Conclusion

The study area lies in "Qantara shark", this area can be considered as the northwestern part of Sinai Peninsula or as the eastern part of the Egyptian delta. The main fresh water aquifer occupied in the Holocene sands to the Pleistocene sand in depth varies from the surface about 0.5 meters. This depth varies according to the cover deposits until reach about 65 m. over sea level in some parts of the study area. Fresh water supply can be related to both of Delta groundwater and the fresh water that runs in the man-made canals of both El-Salam and Prince Gaber.

Saline water which came from integration of sea water underlines the fresh water aquifer about 23 m. to 85 m. according to the cover deposits over the sea level.

7. References

1. Assal, E.M. (1999) Sedimentological studies on the Quaternary sand dunes and sabkhas, northern Sinai, Egypt. M.Sc. Thesis, Geol. Dept., Fac. Sci., Damietta branch, Mansoura Univ., Egypt, 273p.
2. Deiab, A.F. (1998) Geology, pedology and hydrogeology of the Quaternary deposits in Sahl El Tinah area and its vicinities for future development of North Sinai, Egypt. Ph.D. Thesis, Geol. Dept., Fac. Sci., Mansoura Univ., Egypt, 242p.
3. El-Asmar, H.M. (1999) Late Holocene stratigraphy and lithofacies evolution of the Tineh plain, northwestern corner of Sinai, Egypt. Egyptian J. Geol., Vol. 43, No. 2, p: 117-134.
4. Fitterman, D. V., 1986a. Transient electromagnetic sounding in the Michigan basin for groundwater evaluation: presented at National Water Assn. Conference-Surface and Borehole Geophysical Methods. Denver.
5. Fitterman, D. V., and Stewart, M. T., 1986b. Transient electromagnetic sounding for groundwater: Geophysics, 51, 995-1005.

6. Geological Survey of Egypt (GSE), (1992) Geological map of Sinai, A.R.E. Sheet No. 5, Scale 1:250,000.
7. Hoversten G. M., Dey, A. and Morrison H.F., 1982. Comparison of five least-squares inversion techniques in resistivity sounding. Geophysical Prospecting, 30, 688-734.
8. Nabighian, M. N., 1979. Quasi-static response of a conductive half-space. An approximation represntstion. Geophysics, V.44 (10), pp. 1700-1705.
9. RESIST's software, 1990. Manual index of Resist software program.
10. Soliman, M. M. M., 2005. Environmental and geophysical assessment of the ground and subsurface water resources of Ras El-Hekma area, northwestern coast of Egypt. PhD. In Geophysic. Faculty of Science En shams University.
11. Stephan, E. Wendland and Fix. G., 1991. Electromagnetic Modeling by finite element Methods France proceeding
12. TEMIXL XL program V4, 1996. Temix v.4 user's manual, Interpex, 468p.
13. Zohdy, A. A. R., 1989. A new method for automatic interpretation of Schlumberger and Wenner sounding curves; Geophysics, Vol.54, P.244-253